Malaysian Journal of Chemical Engineering & Technology 3 (2) (2020) 11–17

Malaysian Journal of Chemical Engineering & Technology

Journal Homepage: http://myjms.mohe.gov.my/index.php/mjcet

Photocatalytic deposition of silver particles on titania nanotube thin films: Influence of precursor concentration

[a]Lim Ying Pei, [b]Devagi Kanakaraju, [c]Lim Ying Chin*

[a]Faculty of Chemical Engineering, Universiti Teknologi MARA, Selangor, Malaysia
[b]Faculty of Resource Science and Technology, Universiti Malaysia Sarawak, Kota Samarahan, Sarawak
[c]School of Chemistry and Environment, Faculty of Applied Sciences, Universiti Teknologi MARA, Selangor, Malaysia

*Corresponding email: limyi613@uitm.edu.my

Abstract

Titania nanotubes (TiNT) has gained much interest as it has high surface area and fewer grain boundaries. In order to enhance the photoelectrochemical properties of TiNT, modification has been carried out to dope silver on TiNT. In this study, a combination of electrochemical anodisation and a photochemical reduction was employed to fabricate silver supported on titania nanotubes (AgTiNT). TiNT was synthesized via anodisation of titanium plate in a two-electrode system containing ethylene glycol and ammonium fluoride. Then, the silver particles were deposited on TiNT by immersion in various concentrations of silver precursor solution followed by ultraviolet light radiation. The prepared samples were characterized using field emission scanning electron microscopy (FESEM) for morphology, x-ray diffractometry (XRD) for crystal structure and energy dispersive x-ray (EDX) to determine the element content. TiNT demonstrated a well-ordered structure, but the nanotubes tend to clump together upon deposition of Ag. The effect of Ag deposition on the photoelectrochemical performance of TiNT was studied where almost one-fold enhancement in the photoelectrochemical property was observed for AgTiNT compared to pure TiNT.

Article Info

https://doi.org/10.24191/mjcet.v3i2.10943

Article history:

Received date: 7 October 2020
Accepted date: 30 November 2020

Keywords:

Titania
Nanotube
Anodisation
Photochemical
Silver

1.0 Introduction

Titanium dioxide (TiO_2) based composite materials have been extensively investigated due to their unique properties, wide application in the field of photocatalytic, photovoltaic, bio-coating, and photoelectric (Abdullah & Kamarudin, 2017; Hilario et al., 2017; Su et al., 2015; Zhao et al., 2016). However, pristine titanium dioxide has some drawbacks such as large bandgap energy, i.e., 3.2 eV for anatase and fast recombination rate of the photogenerated electron-hole pairs. As such, most of the applications related to TiO_2 can only be activated by UV light, which only accounts for 5% of the solar spectrum. This results in the reduced practical application of TiO_2. In addition, the rapid recombination of photogenerated electron-hole pairs lowered the quantum efficiency. Therefore, in order to overcome this problem, great deals of attempts have been conducted to increase the photo response of TiO_2 into the visible light region and separate the charge carriers effectively by various surface modifications (Fiorenza et al., 2019; Wang et al., 2020; Kanakaraju et al., 2020; Yang et al., 2018). For instance, bandgap engineering through metal or nonmetal doping and dye sensitisation had been adopted to narrow down the bandgap energy of TiO_2 towards visible light region (Montoya & Gillan, 2018; Basavarajappa et al., 2020). However, the reaction set up is costly and there is leaching of dye during photocatalytic reaction. Another drawback of using metal doped photocatalyst is that they are prompt to photo corrosion and thus hampered the photoelectrochemical performance of the samples. One of the efficient ways to boost its photochemical performance is too complex TiO_2 with noble metal. It has been recognized that specific interactions between TiO_2 and noble metal nanoparticles form Schottky barriers which could significantly prohibit the recombination of charge carriers (Brook et al., 2007). Among the noble metal such as platinum (Pt), palladium (Pd) or silver (Ag), Ag is one of the most suitable candidates for industrial application due to its

non-toxicity and ease of preparation.

It was reported that the loading of Ag nanoparticles might enhance the overall photoelectrochemical and photocatalytic performance of TiO_2. Upon light illumination, photo-induced electron-hole pairs are generated. The Ag nanoparticles not only act as photo sensitizer but also act as sinks for photogenerated electrons and thus decrease the recombination of these charge carriers (He et al., 2002). Therefore, there will be more charge carriers that could involve in the redox reaction and enhance the photocatalytic/photoelectron-chemical efficiency. In addition, Ag nanoparticles on the surface of TiO_2 could exhibit a characteristic surface plasmon band under visible due to the collective excitation of surface electrons in Ag nanoparticles (Gao et al., 2013). For example, Wang et al. (2016) prepared Ag modified TiO_2 and found that the nanocomposite showed higher photo-electrocatalytic decomposition efficiencies of azo dyes.

Loading of Ag nanoparticles onto TNT could be accomplished by chemical reduction, sputtering deposition, microwave-assisted method in which additional chemicals, high temperature or post treatments are required during the synthesis process. Herein, we described a simple way to synthesize Ag supported on TiO_2 nanotubes (AgTiNT) using an anodisation coupled photoreduction method as this method offers good control of the structure and morphology of the produced Ag/TNT at room temperature. The effect of $AgNO_3$ concentration on the formation and photoelectrochemical performance of AgTiNT was investigated and discussed.

2.0 Methodology

2.1 Fabrication of silver supported on titania nanotube

The procedure to prepare titania nanotubes (TiNT) were adapted from Harun et al. (2017) with some modifications. Briefly, titanium foil (0.127 mm thickness, 97 % purity, Sigma Aldrich) was cut into 0.9×5 cm^2. The foil was mechanically polished and then cleaned by sonication in acetone, isopropanol and deionized water for 15 minutes prior to anodisation. All the experiments were carried out in a dual-electrode chamber cell where the two electrodes were placed 2 cm apart with constant voltage (20 V) for an hour at room temperature. Titanium foil was used as the anode while high density graphite as the counter electrode. A direct current power supply (Mini Consort) was used as a source of constant voltage. The electrolyte used was 10 vol.% H_2O, 90 vol.% ethylene glycol ($C_2H_6O_2$) and 0.25 wt.% ammonium fluoride (NH_4F). The stirrer waves used for agitation of the electrolyte during the anodisation process aimed to improve the quality of TiNT by uniformly mixing the electrolyte. The samples were then calcined at 500°C for 2 hours in the air. The prepared TiNT was used as a substrate for the deposition of Ag. TiNT was immersed into silver nitrate ($AgNO_3$) solution with a vertically slanting position in various concentrations of $AgNO_3$ solution ranging from 5 mM to 1000 mM for 4 hours and irradiated with an ultraviolet lamp (8 W) for 2 hours at room temperature producing AgTiNT. AgTiNT sample was denoted as xAgTiNT with x represent the concentration of $AgNO_3$ used.

2.2 Characterisation of titania nanotube arrays

Crystal phase identification was carried out using an X-ray diffractometer (XRD, Shimadzu D6000) with Cu Kα radiation (λ= 1.5406 Å). The accelerating voltage and applied currents were 40 kV and 30 mA, respectively. Field Emission Scanning Electron Microscope (FESEM), Carl Zeiss Supra 40 VP was used to analyse the surface morphology of TiNT. A low electron beam voltage of 5 kV was used and therefore, no coating of the sample is required prior to imaging. Energy dispersive analysis of X-ray (EDX) was performed on JOEL JSM 7500F Field Emission Scanning Electron Microscope attached with the Oxford INCA Energy 200 EDX to determine the purity and elemental composition in calcined thin films before and after photoreduction in $AgNO_3$.

2.3 PEC measurement of silver supported on titania nanotubes

The photoelectrochemical behaviour of the TiNT and AgTiNT electrode was evaluated by a transient photocurrent curve. The measurement was carried out using a standard three-electrode configuration: a platinum wire was used as a counter electrode, Ag/AgCl as a reference electrode and the prepared TiNT and AgTiNT as a working photoanode on an electrochemical workstation (AUTOLAB). The photoanode was illuminated by a 120V 300 W halogen lamp with an intensity of 150 mW/cm^2. Photocurrent spectra were acquired in 0.5M Na_2SO_4 solution at a potential of 500 mV (vs. Ag/AgCl).

3.0 Results and discussion

Titania nanotubes were prepared by anodisation of Ti at 20 V in an ethylene glycol solution containing 0.25 wt.% NH_4F. The growth of TiNT was evaluated by monitoring the current versus time curve generated during the anodisation process as shown in Fig. 1.

The drop in current density is due to reduced electroconductivity of the oxide layer on Ti. This event can be presented through the Eq. (1), as shown below:

$$Ti + 2H_2O \rightarrow TiO_2 + 4H^+ + 4e^- \quad (1)$$

The current density increased slightly as shown in Fig. 1. This increase is due to the formation of pores and the initial formation of TiO_2 nanotubes, which are caused by fluoride-induced chemical dissolution of the previously formed TiO_2 (Eq. 2).

$$TiO_2 + 6F^- + 4H^+ \rightarrow [TiF_6]^{2-} + 2H_2O \quad (2)$$

The continued oxidation brings to a higher field-effect at the bottom of the pores and field-assisted dissolution where Ti metal ions will etch from the metal and dissolved in solution. Lastly, the plateau is reached and was represented by the equivalence of pore growth rate at the bottom of the pores with the chemical etching rate of the oxide film at the oxide electrolyte interface (top part of the pores), which leads to the tube formation (Sun et al., 2017).

Fig. 2 depicts the colour change of the as-anodized TiNT film and the corresponding AgTiNT samples Initially, the Ti plate has a shiny surface after ultrasonication. During the anodisation process, the Ti surface was visibly changed to blue, yellow, pink and dark grey colours due to the interference occurs between the reflected ray from the oxide surface and that of the interface of the oxide and the titanium substrate. After anodisation, the TiNT film was immersed into a different concentration of $AgNO_3$ ranging from 5 mM to 1000 mM under UV light illumination. Apparently, the colour of the AgTiNT samples changes with increasing $AgNO_3$ concentration. The film appears darker with a higher concentration of $AgNO_3$; indicating a higher amount of silver was deposited on the TiNT surface.

The crystalline form of TiNT film prepared by electrochemical anodisation was explored using XRD. Fig. 3 shows the XRD patterns of the calcined TiNT and AgTiNT after photoreduction in different concentration of $AgNO_3$.

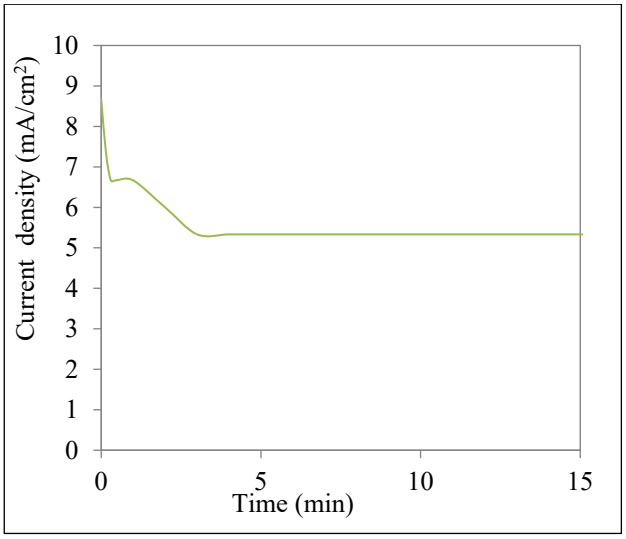

Fig. 1: Characteristics of current density versus time curve obtained during anodisation

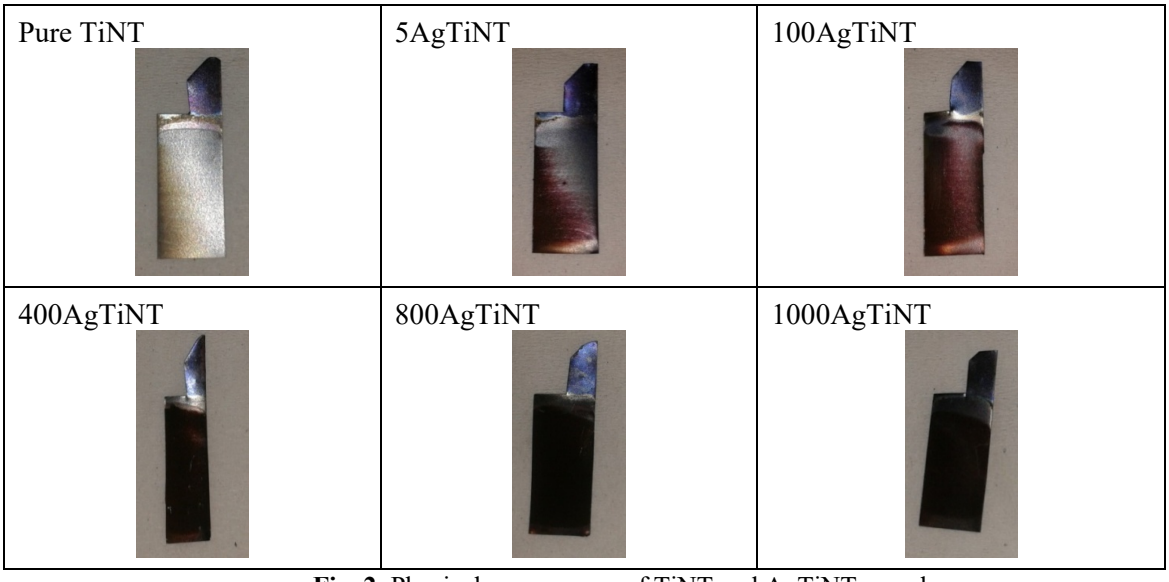

Fig. 2: Physical appearances of TiNT and AgTiNT sample

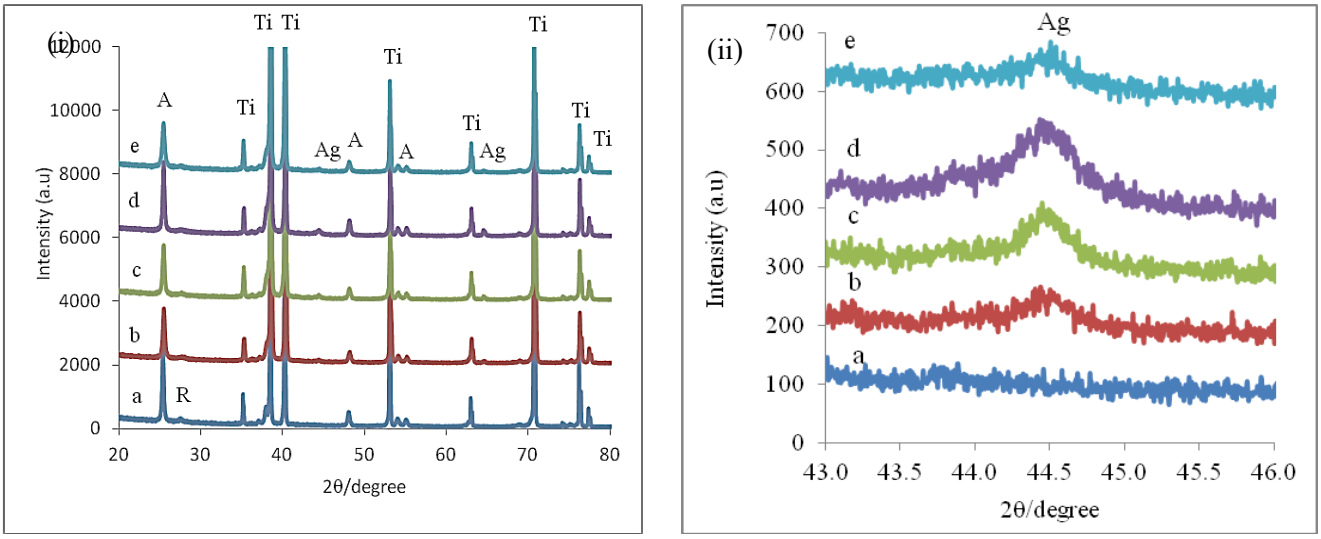

Fig. 3: i) XRD patterns of (a) calcined TiNT and AgTiNT prepared using different concentration of (b) 5AgTiNT (c) 100AgTiNT (d) 400 AgTiNT and (e) 800 mM AgTiNT. A, R, Ti and Ag represent anatase, rutile, titanium and silver, respectively. Fig. 3 (ii) is the magnifying view of XRD patterns at 2θ = 43–46°

The as-anodised samples were amorphous initially. A mixture of anatase and rutile was obtained for all samples upon calcination at 500 °C. The peaks at 2θ = 25.3°, 48.3°, 53.9° and 55.1° correspond to the anatase peak and were well indexed with JCPDS No. 021-1272 and a very weak diffraction peak at 2θ = 44.1° was assigned to rutile (JCPDS No. 00-021-1276).

Peaks at 2θ = 35.4°, 38.4°, 40.2°, 53.2°, 63.0°, 70.7°, 76.2° and 77.4° correspond to the Ti peak (JCPDS No. 00-044-1294). The Ti peaks were from the substrate used for anodisation. The high intensity of the peak showed that the samples were highly crystalline. On contrary, one can observe new metallic Ag peaks at 2θ = 44.4° and 64.5°, corresponding to (200) and (220) diffraction plane in the XRD patterns for all AgTiNT samples which were well indexed to JCPDS 04-0783. This confirmed the existence of Ag within the TiNT matrix. Ultimately, the presence of Ag did not modify the position of the anatase (101) phase at 2θ = 25.4°, revealing that Ag was not weaved into the TiO_2 lattice. In addition, from the magnifying view of XRD patterns in Fig. 3 (ii), the intensities of the Ag peak at 2θ = 44.4° increases from 5 mM to 400 mM, suggesting the amount of Ag incorporated onto TiNT increase with $AgNO_3$ concentration. This observation was then proven from the EDX analysis which will be discussed later.

The FESEM images of AgTiNT prepared at various precursor concentrations were shown in Fig. 4. From Fig. 4a, pure TiNT demonstrated a highly dense and well-ordered appearance with an average diameter of 67 nm and an average tube length of 3.3 µm. The crystalline TiNT was used as a substrate for Ag deposition. Fig. 4(b-f) shows the FESEM images of AgTiNT formed in various concentrations of $AgNO_3$ solution. For 5AgTiNT and 100AgTiNT, the nanotubes started to clump and showed less ordering and with less regularity compared to that of pure TiNT. After immersion in 400 mM and 800 mM $AgNO_3$, more severe clumping of TiNT was observed, indicating that the deposition of Ag particle into the nanotubes has an effect on the morphology of nanotubes. AgTiNT could be seen as more clustered with a higher exposure of the deeper of the film and this increases the surface roughness of the film, which could be beneficial for surface-related applications such as photocatalysis.

The element distribution of AgTiNT was examined by EDX and is shown in Fig. 5. From the EDX mapping analysis, the distribution of titanium and oxygen is almost the same, suggesting that the loading of Ag onto TiO_2 has no effect on the stoichiometric ratio of TiO_2. The EDX mapping revealed that silver particles were deposited homogeneously on the surface of the nanotubes (top part of the pore).

Table 1: Element composition of TiNT and AgTiNT.

Samples	Element (atomic %)		
	Ti	O	Ag
Pure TiNT	33.6	66.4	Not detected
5AgTiNT	30.0	69.0	1.0
100AgTiNT	30.2	67.6	2.2
400AgTiNT	29.5	65.5	5.0
800AgTiNT	31.3	65.0	3.7
1000AgTiNT	30.9	65.5	3.6

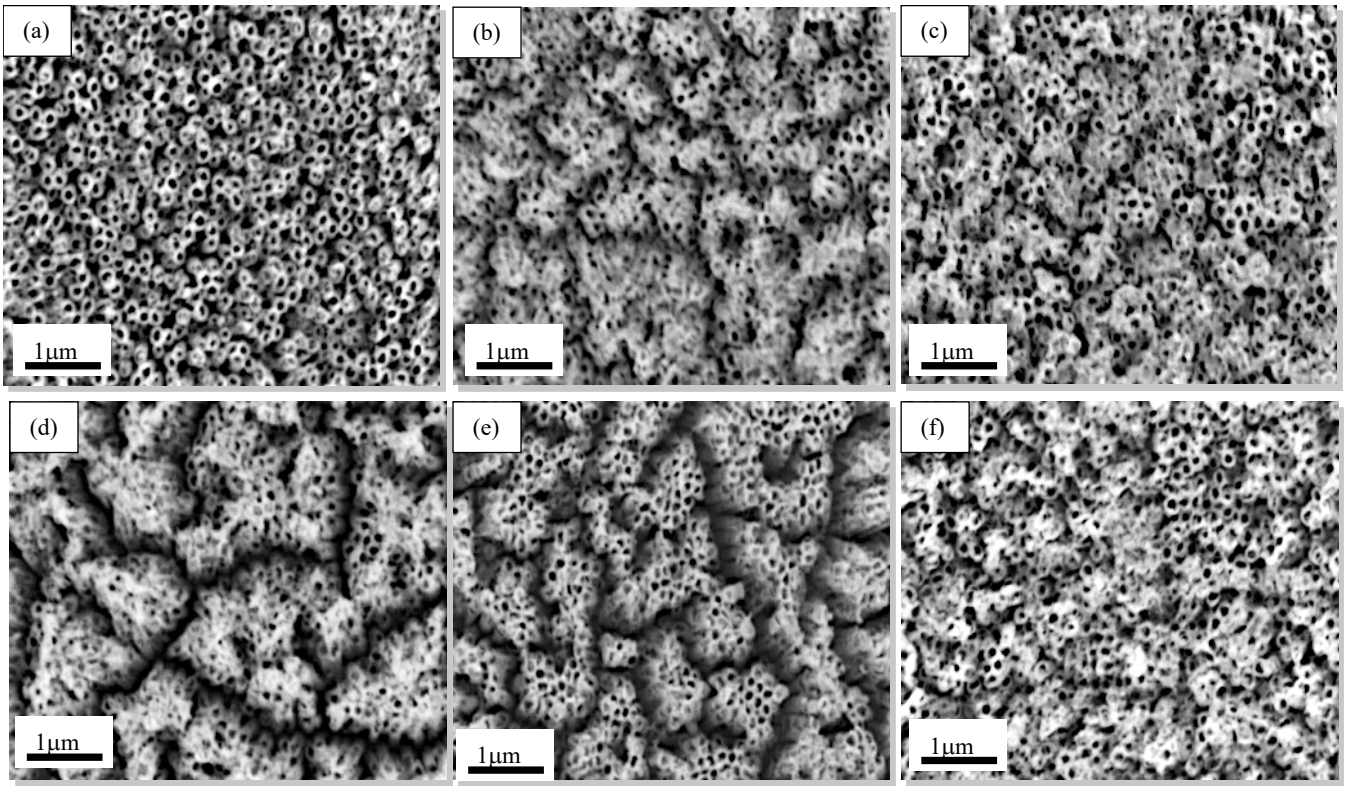

Fig. 4: FESEM images of (a) calcined TNT, (b) 5AgTiNT, (c) 100AgTiNT, (d) 400AgTiNT, (e) 800AgTiNT, and (f) 1000AgTiNT

Table 1 shows the element contents of TiNT and all AgTiNT samples. All samples consist mainly of titanium and oxygen which was originated from titanium dioxide nanotubes. From Table 1, the amount of silver increases with the increasing concentration of silver nitrate.

However, the amount of silver deposited decreases slightly when there is a too high amount of silver ions present in the solution (>800 mM). One possible reason could be the deposition amount was affected by the distance of the sample from the UV light source during photoreduction. As the sample was placed in the order of increasing concentration during photoreduction, thus, the amount of UV light received for each sample to reduce silver ions into silver metal could be somewhat different. TNT that was placed in 400 mM AgNO3 was illuminated with a relatively higher amount of UV light compared to other samples which were placed slightly further away from the UV source.

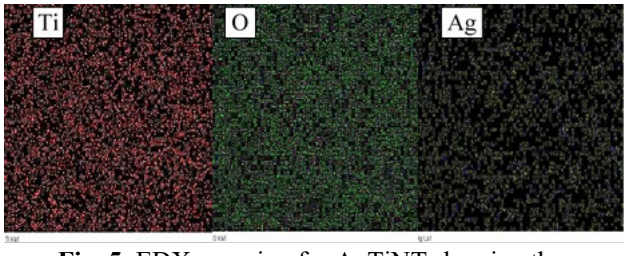

Fig. 5: EDX mapping for AgTiNT showing the distribution of Ti, O, and Ag

Nevertheless, the amount of silver ions that could be reduced and deposited onto TiNT has reached almost constant value (~3.7 at%), revealing a saturation state has been achieved.

Fig. 6 shows the transient photocurrent curve of TiNT and AgTiNT photoelectrodes under halogen lamp illumination. Both the pristine TiNT and AgTiNT samples demonstrated immediate response towards three light on-light off illumination cycles, indicating good adherence of samples towards the substrate (Ti foil) and good quality of the TiNT and AgTiNT film.

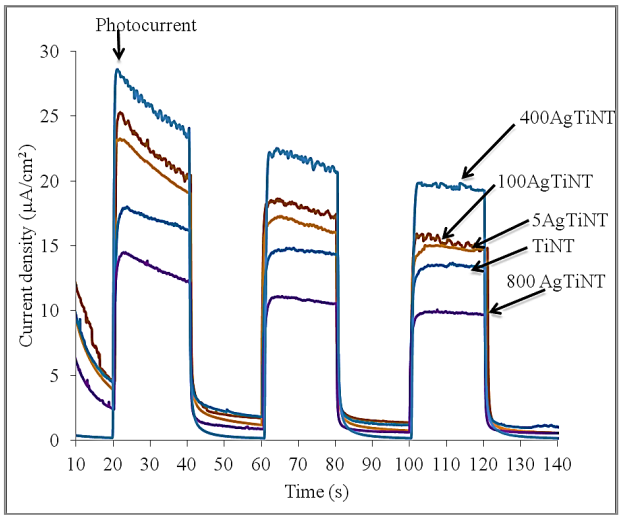

Fig. 6: Transient photocurrent curve for TiNT and AgTiNT photoelectrode under halogen lamp illumination

All the AgTiNT samples exhibited stronger photocurrents compared to pure TiNT electrode except for 800AgTiNT. The highest photocurrent of 27 μA/cm^2 was obtained for 400 AgTiNT, which is 1.7 higher than that of pure TiNT (16 μA/cm^2). The higher photocurrent indicates that more photo-induced electrons can be efficiently transferred from AgTiNT to the counter electrode via an external circuit, resulting in high photoelectrochemical activity. The increases of photocurrent densities are mainly attributed to the visible light absorption by surface plasmon resonance effect of Ag nanoparticles on TiNT. A similar finding was made by Wang et al. (2014) where photocurrent increases with increasing concentration of $AgNO_3$ solution up to 10 mM for AgTiNT prepared via chemical bath deposition. However, another study conducted by Xu et al. (2014) found a contrary result in lower photocurrent in buffer solution for AgTiNT fabricated via photoreduction method. A superior photoelectrochemical performance of 2 mA/cm^2 was demonstrated by AgTiNT produced by hydrothermal method. Nevertheless, the synthesis route required high temperature of 180 °C for 12 hours (Zhong et al. 2015).

4.0 Conclusions

In summary, well-aligned TiO_2 nanotube was successfully synthesized by anodisation of Ti foils, and then Ag nanoparticles were decorated on the surface of the nanotubes through a photoreduction method. The result shows that the amount of silver deposited increased with increasing concentration of $AgNO_3$ up to 400 mM. Ag nanoparticles deposition on the TNT resulted in almost one-fold enhancement of the photoelectrochemical performance compared to bare TNT. The sensitisation of TiO_2 nanotubes by silver particles modified the morphology of the nanotubes and consequently enhanced the visible light response of the doped samples. This study demonstrates potential application of silver doped titania nanotubes as photoanode for solar energy conversion devices.

Acknowledgement

This work is financially supported by Universiti Teknologi MARA, through the GIP Grant (600-IRMI/ 5/3/GIP (025/2018).

References

A.T. Montoya, E.G. Gillan, (2018). Enhanced Photocatalytic Hydrogen Evolution from Transition-Metal Surface-Modified TiO_2, *ACS omega*. *3*. 2947–2955.

C. He, Y. Yu, X. Hu, A. Larbot, (2002). Influence of Silver Doping on The Photocatalytic Activity of Titania Films, *Applied Surface Science. 200.* 239–247.

D. Kanakaraju, M.H. bin Ya, Y.C. Lim, A. Pace, (2020). Combined Adsorption/Photocatalytic Dye Removal by Copper-Titania-Fly Ash Composite, *Surfaces and Interfaces*. 100534.

F. Hilario, V. Roche, R. P. Nogueira & A. M. J. Junior, (2017). Influence of Morphology and Crystalline Structure of TiO_2 Nanotubes on Their Electrochemical Properties and Apatite-Forming Ability. *Electrochimica Acta.* 337–349.

G. Xu, H. Liu, J. Wang, J. Lv, Z. Zheng, Y. Wu, (2014). Photoelectrochemical Performances and Potential Applications of TiO_2 Nanotube Arrays Modified with Ag and Pt nanoparticles, *Electrochimica Acta*. 194–202.

H. Wang, J. Lu, L. Liu, W. Cui, Y. Liang, (2020). Ultra-thin rGO Nanosheet Modified TiO_2 Nanotube Arrays for Boosted Photoelectrochemical Performance, *Applied Surface Science.* 144966.

J. Zhong, Q. Wang, Y. Yu, (2015). Solvothermal Preparation of Ag Nanoparticles Sensitized TiO2 Nanotube Arrays with Enhanced Photoelectrochemical Performance, *Journal of Alloys and Compounds.* 168–171.

L. Brook, P. Evans, H. Foster, M. Pemble, A. Steele, D. Sheel, H. Yates, (2007). Highly Bioactive Silver and Silver/Titania Composite Films Grown by Chemical Vapour Deposition, Journal of Photochemistry and Photobiology A: *Chemistry. 187*. 53–63.

M. Abdullah & S. K. Kamarudin, (2017). Titanium Dioxide Nanotubes (TNT) in Energy and Environmental Applications: An Overview. *Renewable and Sustainable Energy Reviews*. 212–225.

N.F.A. Harun, Y. Mohd, Y.P. Lim, C.Y. Yin, Y.C. Lim, (2018). Understanding the Characteristics, Enhanced Optical and Photoelectrochemical Performance of Copper-Loaded Titania Nanotubes Synthesized via Successive Ionic Layer Adsorption Reaction, *Journal of Materials Science: Materials in Electronics.* 14210–14221.

P. Su, H. Li, J. Wang, J. Wu, B. Zhao, & F. Wang, (2015). Facile Preparation of Titanium Dioxide Nano-Capsule Arrays Used as Photo-Anode for Dye Sensitized Solar Cells. *Applied Surface Science*. 636–642.

P.S. Basavarajappa, S.B. Patil, N. Ganganagappa, K.R. Reddy, A.V. Raghu, C.V. Reddy, (2020). Recent Progress in Metal-doped TiO_2, Non-metal Doped/codoped TiO_2 and TiO_2 Nanostructured Hybrids for Enhanced Photocatalysis, *International Journal of Hydrogen Energy. 45*. 7764–7778.

Q. Wang, J. Zhong, M. Zhang, D. Chen, Z. Ji, (2016). In Situ Fabrication of TiO_2 Nanotube Arrays Sensitized by Ag Nanoparticles for Enhanced Photoelectrochemical Performance. *Materials Letters.* 163–167.

R. Fiorenza, S. Sciré, L. D'Urso, G. Compagnini, M. Bellardita, L. Palmisano, (2019). Efficient H2 Production by Photocatalytic Water Splitting Under UV or Solar Light Over Variously Modified TiO_2-Based Catalysts, *International Journal of Hydrogen Energy. 44.* 14796–14807.

T. Yang, J. Peng, Y. Zheng, X. He, Y. Hou, L. Wu, X. Fu, (2018). Enhanced Photocatalytic Ozonation Degradation of Organic Pollutants by ZNO Modified TiO_2 Nanocomposites, *Applied Catalysis B: Environmental.* 221. 223–234.

Y. Gao, P. Fang, F. Chen, Y. Liu, Z. Liu, D. Wang, Y. Dai, (2013). Enhancement of stability of N-doped TiO2 Photocatalysts with Ag Loading, *Applied Surface Science.* 796–801.

Y. Sun, Q. Zhao, G. Wang & K. Yan, (2017). Influence of Water Content on the Formation of TiO2 Nanotubes and Photoelectrochemical Hydrogen Generation. *Journal of Alloys and Compounds.* 514–520.

Y. Wang, Z. Li, Y. Tian, W. Zhao, X. Liu, J. Yang, (2014). Facile Method for Fabricating Silver-Doped Tio2 Nanotube Arrays with Enhanced Photoelectrochemical Property, *Materials Letters*. 248–251.

Y. Zhao, N. Hoivik & K. Wang, (2016). Recent Advance on Engineering Titanium Dioxide Nanotubes for Photochemical and Photoelectrochemical Water Splitting. *Nano Energ.* 728–744.